bioRxiv preprint doi: https://doi.org/10.64898/2025.12.22.696002; this version posted December 25, 2025. The copyright holder for this preprint (which was not certified by peer review) is the author/funder. All rights reserved. No reuse allowed without permission.

Guam amyotrophic lateral sclerosis/parkinsonism-dementia complex (ALS/PDC) features CTE-like tau seeds in brain and spinal cord

Nil Saez-Calveras[a,b,#], Bert M. Verheijen[c,#,*], Nabil Morgan[a], Elizabeth Hill[a], Skyler Taylor[a], Kiyomitsu Oyanagi[d], Akiyoshi Kakita[e], Yuyu Song[f], Lukasz A. Joachimiak[a], Jaime Vaquer-Alicea[a], Marc I. Diamond[a,§], Ying Lu[c,§,*]

[a]Center for Alzheimer's and Neurodegenerative Diseases, Peter O'Donnell Jr. Brain Institute, University of Texas Southwestern Medical Center, Dallas, TX, USA

[b]Department of Neurology, University of Texas Southwestern Medical Center, Dallas, TX, USA

[c]Department of Systems Biology, Harvard Medical School, Boston, MA, USA

[d]Division of Neuropathology, Department of Brain Disease Research, Shinshu University School of Medicine, Matsumoto, Nagano, Japan

[e]Department of Pathology, Brain Research Institute, Niigata University, Niigata, Japan

[f]Department of Neurology, Massachusetts General Hospital, Boston, MA, USA

[#]Contributed equally to this work
[§]Co-senior author

*Corresponding author
Email: lambertus_verheijen@hms.harvard.edu; ying_lu@hms.harvard.edu

Competing Interest Statement: The authors declare no competing interest.

Keywords: amyotrophic lateral sclerosis-parkinsonism dementia complex (ALS/PDC); neurodegenerative disease; tau; seeding; alanine scan

bioRxiv preprint doi: https://doi.org/10.64898/2025.12.22.696002; this version posted December 25, 2025. The copyright holder for this preprint (which was not certified by peer review) is the author/funder. All rights reserved. No reuse allowed without permission.

Abstract

Amyotrophic lateral sclerosis/parkinsonism-dementia complex (ALS/PDC) is a fatal neurodegenerative disorder that was once hyperendemic in the island of Guam (Mariana Islands, US) and a few other Pacific locales. Despite extensive investigations into its origins, the etiology of ALS/PDC remains unclear. ALS/PDC is, at the neuropathology level, characterized by tau-dominant multiple proteinopathy in brain and spinal cord. It was recently reported that Guam ALS/PDC brain extracts exhibit tau seeding activity in fluorescence resonance energy transfer (FRET)-based biosensor cells. To build upon those findings and explore the nature of tau seeds in ALS/PDC in more detail, we used an alanine mutational scanning (Ala scan) approach to determine the seeding profile of tau in nervous tissues of Guam ALS/PDC cases. First, we confirmed the detection of tau seeding activity in ALS/PDC brain samples in tau biosensor cells. Notably, we could also detect potent tau seeding activity in spinal cord. Subsequent Ala scan assays demonstrated that ALS/PDC tau displays an aggregate incorporation pattern that resembles that of chronic traumatic encephalopathy (CTE)-type tau. This result is consistent with recent electron cryo-microscopy studies of tau, which revealed that ALS/PDC tau filaments are predominantly of the CTE-type. The structural characteristics and seeding behavior of ALS/PDC tau, as well as the regional distribution of tau pathology at post-mortem, suggest that ALS/PDC is a CTE-like tauopathy.

bioRxiv preprint doi: https://doi.org/10.64898/2025.12.22.696002; this version posted December 25, 2025. The copyright holder for this preprint (which was not certified by peer review) is the author/funder. All rights reserved. No reuse allowed without permission.

Significance Statement

Neurodegenerative tauopathies are characterized by proteinaceous deposits containing microtubule-associated tau in nervous tissue. Emerging evidence suggests that disease-associated tau proteins adopt abnormal, self-propagating conformations characteristic of prions. Here, we employed alanine mutational scanning (Ala scan) to determine the nature of prion-like tau seeds in ALS/PDC, a mysterious disorder that occurred formerly in high incidence in certain regions in the western Pacific. We show that the Ala scan incorporation profile of ALS/PDC tau is similar to that of abnormal tau proteins in chronic traumatic encephalopathy (CTE). The findings lend support to the idea that ALS/PDC can be classified structurally as a CTE-like tauopathy. This work may have important implications for our understanding of ALS/PDC as well as common neurological disorders beyond the Pacific.

bioRxiv preprint doi: https://doi.org/10.64898/2025.12.22.696002; this version posted December 25, 2025. The copyright holder for this preprint (which was not certified by peer review) is the author/funder. All rights reserved. No reuse allowed without permission.

Main Text

Introduction

Amyotrophic lateral sclerosis/parkinsonism-dementia complex (ALS/PDC) is a rare neurodegenerative disorder of unknown cause that previously occurred in high incidence in the Pacific Island of Guam (Mariana Islands, US) (1-5) as well as other geographic foci in the western Pacific, i.e., the Kii peninsula of Japan (6, 7) and the southern coastal region of Papua (8, 9). The disease presents clinically as progressive motor neuron disease (ALS), parkinsonism with dementia (referred to as parkinsonism–dementia complex or PDC), or a combination thereof. Pacific ALS appears to be similar to ALS occurring elsewhere. PDC, however, seems to be a unique disorder found only in the western Pacific.

Research into ALS/PDC has been primarily stimulated by hypotheses as to cause. It was once hoped that understanding the cause of ALS/PDC in the Pacific isolates would provide insight into analogous neurological disease encountered throughout the world (e.g., idiopathic ALS). We will concentrate here on the Guam cluster of disease, i.e., the focus that harbors the most intensively studied ALS/PDC variant. Although various causes have been proposed for ALS/PDC in Guam, such as genetic factors, infections, and exposure to toxins, no conclusive evidence has been found for any of those (10). A remarkable decrease in disease incidence has been seen with increased westernization (11, 12) and migration studies have indicated that the disease could also develop after long-term residence in Guam (13). These observations hint at some role for exogenous factors in ALS/PDC etiopathogenesis.

At the neuropathology level, Guam ALS/PDC is characterized by widespread neurofibrillary tangles (NFTs) composed of hyperphosphorylated microtubule-associated tau protein (14-16), often in combination with other protein abnormalities, e.g., intracytoplasmic phospho-TAR DNA-binding protein of 43 kDa (pTDP-43) aggregates (17-19) (**Fig. S1**). Protein aggregates are found in brain and spinal cord tissues, in both neurons and glial cells in gray and white matter (20-25). NFTs in ALS/PDC brains are composed of all six tau isoforms (3R + 4R) and are prominent in superficial cortical layers, i.e., cortical layers II/III (26). Of note are the occurrence of granular/fuzzy astrocytes and subpial thorn-shaped astrocytes localized in the depth of cortical sulci (27). α-synucleinopathy can also be occasionally observed (28-30), but β-amyloid (Aβ) plaques are mostly absent and are not considered a defining feature of ALS/PDC [a summary of neuropathology can be found in reference (31)]. It has been reported that NFTs are also frequently present in nervous tissues of Guam non-neurological control subjects at post-mortem (32, 33), likely indicating a presymptomatic state. It is conceivable that shared genetic risk and/or exposure to a common etiologic agent resulted in a certain degree of background pathology in the Guam populace. ALS/PDC cases in the Kii cluster show neuropathological features that are largely comparable to those in Guam ALS/PDC (34). No necropsies were performed on ALS/PDC cases in the Papua cluster and it is therefore unknown whether those cases are neuropathologically similar to ALS/PDC in the other geographic isolates.

A growing body of evidence suggests that tau can adopt disease-specific pathological conformations that spread through the nervous system by a prionic mechanism to cause diseases like Alzheimer's disease (AD) and other tauopathies (35-37). According to this model, structurally distinct tau conformers replicate by inducing the templated conversion of native tau proteins into pathological forms ("seeding") and produce predictable patterns of pathology, akin to prion strains. Faithful propagation of abnormal tau has been demonstrated in both cell and mouse models (38-41). Insight into the precise nature of different tau strains and their association with different tauopathies could lead to a better understanding of the molecular mechanisms underlying disease as well as the development of improved diagnostics and

bioRxiv preprint doi: https://doi.org/10.64898/2025.12.22.696002; this version posted December 25, 2025. The copyright holder for this preprint (which was not certified by peer review) is the author/funder. All rights reserved. No reuse allowed without permission.

therapies (42). Recent work has shown that Guam ALS/PDC brain extracts display tau seeding activity in fluorescence resonance energy transfer (FRET)-based biosensor cells (43). Additionally, electron cryo-microscopy (cryo-EM) analysis of tau filaments isolated from ALS/PDC nervous tissues has shown that abnormal tau in these cases is structurally similar or identical to the tau found in chronic traumatic encephalopathy (CTE), a disease associated with repetitive brain trauma (44, 45). This particular tau fold has thus far also been observed in subacute sclerosing panencephalitis (SSPE), a rare consequence of measles virus infection (46), and in vacuolar tauopathy (VT), a form of dementia caused by mutation in the gene encoding valosin-containing protein (*VCP*) (47). The tau amyloid structure itself appears to encode information required to establish unique patterns of disease and it will therefore be of considerable interest to further explore the characteristics of conformationally diverse disease-associated tau species.

In the present study, we used an alanine mutational scanning (Ala scan) approach (48) to determine the seeding signature of tau in Guam ALS/PDC cases. This strategy relies on a prion species barrier concept for tau, i.e., the notion that specific abnormal tau assemblies cannot serve as a template for native tau monomers if the amino acid sequences are incompatible. By sequentially mutating each residue in the repeat domain (RD) of tau (corresponding to the core of the tau protein that is responsible for its aggregation) to a functionally neutral alanine, an incorporation profile of tau can be established through cytometry-based seeding experiments. It has been demonstrated that Ala scan can robustly discriminate between different tau strains (48, 49). We find that, when compared to other tauopathy profiles, ALS/PDC tau seeding profiles resemble those of CTE-type tau. This is in agreement with the reported atomic-level cryo-EM structures of ALS/PDC tau (44). Thus, the data supports the structure-based classification of Guam ALS/PDC as a CTE-like tauopathy.

bioRxiv preprint doi: https://doi.org/10.64898/2025.12.22.696002; this version posted December 25, 2025. The copyright holder for this preprint (which was not certified by peer review) is the author/funder. All rights reserved. No reuse allowed without permission.

Results

FRET biosensor cells detect tau seeds in ALS/PDC brain and spinal cord tissues

We included 14 ALS/PDC cases (Age: 61.07, SD 9.75; M:F 2.5:1) as well as 8 control cases (Age: 52.75, SD 16.46; M:F 3:1), the latter corresponding to Guam subjects that did not develop symptomatic disease. An overview of all tissue samples used in this study can be found in **Table 1** and the **Supplementary Information** (this overview also includes identifiers for associated whole-genome sequencing and RNA-sequencing data on these nervous tissues).

To measure tau seeding activity in Guam ALS/PDC and control nervous tissues, we used engineered tau biosensor cell lines that carry constructs genetically encoding the 3-repeat (3R) or the 4-repeat (4R) wild-type tau RD (residues 246-408) fused to the fluorophores Cerulean and Ruby. Three biosensor cell lines were used, one consisting of 3R tau only (3R/3R), one consisting of 4R tau only (4R/4R), and one consisting of a mixture of 3R and 4R tau (3R/4R) (**Fig. 1**). If tissue extract containing seed-competent tau is added to these cells, this will lead to a FRET signal due to incorporation of tau into seeded aggregates, which can be detected by flow cytometry. Samples can exhibit preferential seeding on either the 3R/3R, 3R/4R or 4R/4R biosensors, presumably depending on the isoform composition of the tauopathy homogenates.

We incubated the three biosensor cell lines with brain homogenate from the ALS/PDC cases and controls. We observed that tau seeding of ≥2% could be detected in the 4R/4R biosensors, but not the 3R/3R or 3R/4R biosensors, in the brain (frontal cortex) and spinal cord of a subset of ALS/PDC cases (n=10/14). Tau seeding was detected in 7/12 frontal cortex samples, and 7/9 of the spinal cord samples. Interestingly, select Guam control cases (n=2/8) also showed seeding activity in the biosensor cells, with a similar preference for the 4R/4R biosensors (**Table 1**, **Fig. 2**). Of note, the tau seeding activity may have been limited by tissue availability, as only 3.5 µg of tissue per well in a 96-well plate were used for seeding in the biosensors.

The presence of tau seeds in ALS/PDC brain (frontal cortex) is in agreement with published data (43). To our knowledge, this is the first demonstration of seeding-competent tau in the spinal cord. It should be noted that the mean age of the included Guam control cases (mean age: 52.75) was lower than that of ALS/PDC cases (mean age: 61.07), which may have impacted the outcome of the seeding assays. It is unknown what causes the preference for seeding in the 4R/4R tau biosensors in these cases, but the presence of specific 4R tau species that are more seed-competent or a switch in isoform preference could underlie this effect (48, 50).

Overall, the highest tau seeding activity among all cases tested was found in spinal cord tissue, samples 15 and 37. A case used for previous cryo-EM analysis of tau (sample 17), in which ALS/PDC tau filaments were found to adopt the CTE fold (44), also showed seeding activity. The cases that had ≥2% seeding activity in the seeding reporter cells were selected for tau Ala scan experiments.

Alanine mutational scanning of ALS/PDC tau identifies a CTE-like signature

We next exploited a tau Ala scan functional genetics approach (48) to determine the nature of tau seeds in Guam ALS/PDC. By sequentially introducing alanine substitutions into the tau RD (residues 246-408), the ability of the tau point mutants to incorporate into unique strains will be differentially affected (**Fig. 3**). Identifying the residues required to form each strain's core allows one to "fingerprint" tau strains and precisely distinguish conformationally different

bioRxiv preprint doi: https://doi.org/10.64898/2025.12.22.696002; this version posted December 25, 2025. The copyright holder for this preprint (which was not certified by peer review) is the author/funder. All rights reserved. No reuse allowed without permission.

species (48, 49).

We incubated Guam ALS/PDC nervous tissue extracts with the mutant tau biosensor cells and through flow cytometry analysis were able to extract an incorporation profile (**Fig. 4**). Samples 36 and 37 originated from the same patient, and corresponded to the frontal cortex and spinal cord, respectively. When we compared the Ala scan profiles from these samples with those of other tauopathies, we found that all Guam samples evaluated (n=8, **Table 2**) most closely resembled the profiles seen in CTE with an average R^2 (R^2 Avg) of 0.566 and a SD of 0.037 (**Fig. 5**). Observed correlations against CTE were significantly better than those against AD (R^2 Avg 0.294 +/- SD 0.044), progressive supranuclear palsy (PSP) (R^2 Avg 0.165 +/- SD 0.039), and corticobasal degeneration (CBD) (R^2 Avg 0.226 +/- SD 0.054). We could not extract a profile for all cases that exhibited seeding due to limited tissue availability. When the 8 ALS/PDC profiles were averaged, the mean ALS/PDC profile strongly correlated with CTE (R^2 0.805) (**Fig. 6**).

Cluster analysis confirmed that the Guam ALS/PDC samples show a comparable incorporation profile to CTE i.e., the Guamanian samples clustered together with CTE, when compared to profiles from other tauopathies (**Fig. 7A**). Importantly, the data indicated that ALS/PDC tau seeds are different from AD-type tau seeds, which are known to be structurally similar to CTE-type tau, but have a slightly different (i.e., less “open”) conformation (44, 45). In this analysis, we also included two primary age-related tauopathy (PART) samples, which we had previously found to match the incorporation profile of AD (49). Profiles of some ALS/PDC samples exhibited poor correlation amongst each other (i.e., sample 7 vs. samle 19; sample 3 vs. sample 41), despite exhibiting a robust correlation with the CTE profile (**Fig. 7B**). However, we deem this effect may have been confounded by low seeding activity due to limited tissue availability in these samples, which contributed to an increased background signal in non-residue hit positions.

Overall, our data demonstrates that ALS/PDC tau seeds closely resemble those present in CTE. We therefore propose to classify ALS/PDC as a CTE-type tauopathy.

bioRxiv preprint doi: https://doi.org/10.64898/2025.12.22.696002; this version posted December 25, 2025. The copyright holder for this preprint (which was not certified by peer review) is the author/funder. All rights reserved. No reuse allowed without permission.

Discussion

We report here on the seeding behavior of tau in Guam ALS/PDC, a neurodegenerative disorder of unknown cause that was previously highly prevalent in the Pacific Island of Guam (Mariana Islands). In agreement with a recent publication (43), we found that Guam ALS/PDC brain samples display robust tau seeding activity in tau biosensor cells. Notably, we also detected strong tau seeding activity in spinal cord tissue. To our knowledge, this is the first description of seed-competent tau in spinal cord. The significance of the presence of tau seeds in the spinal cord region is not clear currently, however, tau inclusions in the spinal cord appear to be present in a number of neurological disorders other than Pacific ALS/PDC (23, 51-54). Spinal cord tau pathology may be more widespread and perhaps defines a subset of disease cases. A comprehensive analysis of tau pathology in spinal cord tissues across neurodegenerative diseases, including measurements on tau seeding activity, would provide additional context. Further, we found that 2 out of 8 Guam non-neurological control subjects also showed seeding activity in the biosensor cells. This is in keeping with seeding data from another study (43) and with previous neuropathological findings in Guamanians, i.e., tau pathology appears to be a frequent background feature in the Guam population (32, 33). A plausible explanation is that these tissues represent presymptomatic cases. An alternative, and perhaps more provocative, explanation is that some individuals may possess resilience against tau seeds (43). Another possibility is that the tau seeds detected in our assay may not be a dominant factor in determining disease phenotypes overall. Tau seeds in all evaluated tissues showed a strong preference for the 4R/4R tau biosensors. This preference was also observed in the aforementioned study on tau seeds in Guam ALS/PDC (43). CTE tau appears to also seed preferably onto 4R/4R biosensors (48). It is not clear why Guam ALS/PDC and CTE, which are both 3R + 4R tauopathies, feature tau seeds that prefer to seed on 4R-only tau reporter cells, but a potential explanation is that tau seeds behave like this due to their specific structural conformation. A specific 4R tau species in ALS/PDC may have particularly strong seeding activity. The cellular source from which these tau seeds arise in ALS/PDC is not known.

We selected 8 samples that displayed robust seeding activity in the 4R/4R biosensors (≥2% seeding threshold) and had sufficient tissue availability to perform tau Ala scan assays. We found that all samples analyzed showed an Ala scan incorporation profile that most closely resembled that of CTE-type tau. A consensus ALS/PDC incorporation profile robustly correlated with CTE (R^2 0.805). In accordance with our findings, *Qi et al.* recently reported on the cryo-EM structures of tau filaments in ALS/PDC brain and spinal cord tissues (44), showing that tau filaments in ALS/PDC adopt folds that appear to be identical to those identified in CTE (45), SSPE (46) and VT (47), disorders that are associated with repetitive brain trauma, measles virus infection, and *VCP* mutation, respectively. Cryo-EM has allowed the development of a structure-based classification of tauopathies (36) and provides a basis for categorizing ALS/PDC tau filaments. Like in CTE, two types of tau filaments (Type I and Type II) were present in variable amounts, each with an unknown, internal density in the β-helix of the structured core (44). The unknown density may represent a cofactor for filament formation. Determining the nature of this extra density is not straightforward, because amyloids extracted from human brains contain different types of contaminants that make finding out what specific densities are present difficult. The ALS/PDC (/CTE) tau fold differs from the AD tau fold, because of the more open conformation of the β-helix region. Type I and Type II filaments are both made of two identical protofilaments, with different interprotofilament packing, i.e., Type I and Type II filaments are ultrastructural polymorphs. A third type of tau filament (Type III), in which two protofilaments pack with opposite polarities, was also identified in both CTE and ALS/PDC (44). The classification of ALS/PDC as a CTE-type tauopathy is now further supported by the Ala scan data in this study, which identified a hit pattern closely matching CTE but not AD, PSP or CBD. Interestingly, tau filaments extracted from Kii ALS/PDC tissues

bioRxiv preprint doi: https://doi.org/10.64898/2025.12.22.696002; this version posted December 25, 2025. The copyright holder for this preprint (which was not certified by peer review) is the author/funder. All rights reserved. No reuse allowed without permission.

had identical structures on cryo-EM (44), providing support for the notion that ALS/PDC of Guam and Kii are similar or identical diseases. No Kii ALS/PDC cases were included in the present study, but it would be of interest to analyze tau from those cases in the Ala scan assay in the future. Understanding the cause of ALS/PDC in Guam may provide insight into the cause of Kii ALS/PDC and vice versa. No neuropathological studies are available for the disease cluster in Papua, rendering comparisons of pathology features with that geographic focus of disease impossible at this time. Ala scan of other tauopathies that adopt the CTE-fold, i.e., SSPE and VT, may also reveal similar incorporation profiles. We anticipate that Ala scan of diverse tauopathies will result in a classification scheme that is compatible with the classifications established by cryo-EM, because the tau amyloid structures are coupled to its seeding behavior. This is particularly important for rare tauopathies, such as ALS/PDC, in which tissue availability constitutes a limiting factor and cryo-EM may not be feasible. In this study, we were able to extract a profile for all seeding cases where 1 mg of material was available.

It is important to emphasize that ALS/PDC is a multiproteinopathy that does not only involve tau deposits, but also features other protein abnormalities, such as pTDP-43 inclusions. It has been put forward that Guam ALS/PDC is, in fact, a multi-prion disorder, that involves tau prions as well as other proteopathic seeds, i.e., Aβ prions (43). The detection of Aβ seeds in ALS/PDC brains is somewhat remarkable given the relative absence of extracellular Aβ plaques (55-57) [although a number of studies do report on Aβ deposits in ALS/PDC (58-62), and senile plaques may be more frequent in subjects of advanced age]. Cryo-EM analyses of Guam ALS/PDC cases also found Type II Aβ42 filaments in one tissue sample (44). One possibility is that certain protein seeds can be present in the absence of evident deposits of such proteins on histology (43, 63-66). Attempts to detect α-synuclein seeds in ALS/PDC using biosensor assays were unsuccessful (43), but the most likely brain regions to contain such seeds, i.e., amygdala and cerebellum, were not included in those experiments. Another study did find evidence for α-synuclein seeds in Guam ALS/PDC through seed-amplification assays (67). Methodological differences could underlie these discrepancies. Sampling from different nervous system regions may be required to adequately detect certain seed-competent proteins. Also, select seeds may only be present in a subset of cases. We focused in our experiments on tau seeding, but future studies should investigate the role of other protein seeds (e.g., TDP-43) in more detail, also taking into consideration potential interactions between various pathologies.

Several limitations should be pointed out. First, the number of samples and amounts of tissue included were low. Because of limited availability of tissues, we relied on archival frozen tissue specimens for these experiments. This also meant we were restricted to a limited number of neuroanatomical regions (i.e., frontal cortex and spinal cord). These limitations may contribute to variation observed in our assays. In addition to the low amount of input material available for our assays, differences in sampling and sample processing may have contributed to overall noise in the data. The variation between samples could also be related to the heterogeneity of ALS/PDC itself, which shows considerably variety in presentation.

In summary, in this study we leveraged Ala mutational scanning to determine the incorporation profile of Guam ALS/PDC tau into aggregates. We found that Guam ALS/PDC tau showed an Ala scan incorporation profile that is similar to that of CTE-type tau. Based on this data, and on the cryo-EM structures of ALS/PDC tau as well as observations regarding the regional distribution of tau pathology in ALS/PDC (e.g., laminar selectivity), we suggest to classify ALS/PDC as a CTE-like tauopathy. The findings support the use of the Ala scan assay for rapid and unbiased classification of tauopathies, especially when tissue availability is limited and cryo-EM cannot be performed. Further optimization of the assay, as well as inclusion of other neuroanatomic regions, will help better characterize these disorders.

bioRxiv preprint doi: https://doi.org/10.64898/2025.12.22.696002; this version posted December 25, 2025. The copyright holder for this preprint (which was not certified by peer review) is the author/funder. All rights reserved. No reuse allowed without permission.

Materials and Methods

Human Brain Samples

Post-mortem brain and spinal cord tissue specimens from Guam ALS/PDC cases and Guam controls were used for experiments in this study. Use of human postmortem tissues was approved by the Ethics Committee of Niigata University [2020–0019].

Tissue Processing

Frozen brain tissue samples were suspended in Tris-buffered saline (TBS) containing cOmplete mini protease inhibitor tablet (Roche) at a concentration of 10% weight/volume in a 1.5 ml low-binding tube (Thermo Fisher Scientific). The tissue was homogenized using a handheld homogenizer (BT Lab Systems) for 1 minute in a vented hood. The homogenates were centrifuged at 21,000xg for 20 minutes. The supernatant was collected as the total soluble protein lysate. Protein concentration was measured using a Pierce 660 Assay (Pierce) and the concentration was adjusted to 1 mg/ml. The fractions were aliquoted into low-binding tubes (Thermo Fisher) and frozen at -80 ˚C until further use. Prior to use in the seeding assays, the thawed homogenates were sonicated for 1 minute using a Q500 Sonicator (QSonica).

Tau RD Biosensor Cell Lines

For this study, the following wild-type (WT) human tau repeat domain (RD) HEK293T biosensor cell lines were used for tau seeding assays:

Tau RD 3R/3R Cells: 3R/3R cells harbor the 3-repeat (3R) version of WT human tau RD (residues 246-408) C-terminally fused to mCerulean (Cer) and mRuby (Ruby) fluorescent protein.

Tau RD 3R/4R Cells: 3R/4R cells harbor the 3R version of WT human tau RD (246-408) C-terminally fused to Cer, and 4R tau fused to Ruby.

Tau RD 4R/4R Cells: 4R/4R cells harbor 4R tau fused to Cer and Ruby.

Tau Seeding Assays

Tau RD 3R/3R, 3R/4R and 4R/4R cells were plated into 96-well plates at a density of 20,000 cells per well. After 18 hours, the cells were transduced with a complex of 0.75 µl of lipofectamine 2000 (Invitrogen), 9.25 µl Opti-MEM (Gibco), and 3.5 µg of 10% weight/volume brain homogenate, for a final treatment volume of 13.5 µl per well. The brain homogenate volume was limited by ALS/PDC tissue availability. After 72 hours, the cells were harvested using 0.25% trypsin-EDTA (Gibco) digestion for 5 minutes at 37°C, followed by quenching with Dulbecco's Modified Eagle Medium (DMEM, Gibco), and transferred to 96-well U bottom plates. The samples were then centrifuge for 5 minutes at 1500 rpm, and the pellet was resuspended and fixed in 2% paraformaldehyde (PFA) in Phosphate-buffered saline (PBS, Gibco) for 10 minutes. The cells were centrifuged again, and the pellet resuspended in 150 µl of PBS for flow cytometry analysis.

4R/4R Alanine Scan

For the alanine scan incorporation assay, 4R/4R biosensor cells were plated at a density of 20,000 cells per well into two 96-well plates per case. This was then followed by treatment with the sonicated homogenates for selected ALS/PDC cases, as described above. 48 hours after initial seeding, once seeded aggregates were observed in the biosensor cells by microscopy imaging, the cells on each plate were re-plated into three 96-well plates to generate technical replicates. The cells were then treated with a library of lentivirus harboring tau RD alanine point mutants spanning from positions 246 to 408, and C-terminally conjugated to mEOS3.2. One alanine point mutant construct was added per well, in addition to the appropriate positive (WT tau RD), and negative controls (double proline I277P-I308P tau RD). 72 hours after lentiviral transduction, the cells were harvested and fixed in PFA as described above.

bioRxiv preprint doi: https://doi.org/10.64898/2025.12.22.696002; this version posted December 25, 2025. The copyright holder for this preprint (which was not certified by peer review) is the author/funder. All rights reserved. No reuse allowed without permission.

Flow Cytometry Analysis

The Attune CytPix Flow Cytometer (Thermo Fisher) was used to perform Fluorescence Resonance Energy Transfer (FRET) analysis. The biosensor cells were analyzed by gating for homogeneous side-scatter and forward-scatter. The FRET signal between Cer and Ruby was measured in the Pacific Blue and Qdot605 channels with gating for cells that contained seeded aggregates in the different biosensors (3R/3R, 3R/4R, 4R/4R). For the alanine scan analysis, a subsequent gate was used for cells positive for FITC (non-photoconverted mEOS3.2), which corresponded to seeded cells that had been successfully transduced with the tau RD-Ala-mEOS3.2 point mutants. Within this population, the FRET signal between Cer and mEOS3.2 was measured in the Pacific Blue and AmCyan channels, and a narrow gate of bright cells was drawn to calculate the median fluorescence intensity (MFI) in the AmCyan channel. The MFI of this FRET signal was used as an indicator of the degree of incorporation of each tau RD alanine point mutant into the seeded aggregates in the 4R/4R biosensors. Alanine mutants K274A, T386A, and P397A are excluded from the scan due to low transduction efficiency.

Alanine Scan Incorporation Data Analysis

The FRET MFI values between Cer and mEOS3.2 measured in the AmCyan channel were normalized by plate to prevent batch variation. The tau RD alanine mutants in the N-terminus and the C-terminus of the sequence do not affect incorporation in our assays. Thus, we used the first twenty mutants in the N-terminus, and the last ten mutants in the C-terminus, as well as the minimum MFI in each plate, to normalize the data and obtain the Incorporation Ratio for each residue position. We used the following formula to obtain this:

$$Incorporation\ Ratio = \frac{Residue\ x\ MFI - Minimum\ MFI}{Average\ MFI - Minimum\ MFI}$$

In this formula Residue x MFI is the FRET MFI in AmCyan for each position, Minimum MFI is the minimum FRET value in the scan for each plate, and Average MFI corresponds to the Average MFI for the first 20 residues (on the first plate), or the last 10 residues (on the second plate). The average of three technical replicates per plate was used for downstream analysis.

Data Analysis

The coefficient of determination (R^2) was used to perform a correlation analysis between the ALS/PDC samples and the other tauopathies. Clustered heatmaps were generated using the *pheatmap* package in R, applying Euclidean distance and complete-linkage clustering to both rows and columns. A custom color scale spanning $R^2 = 0–1$ was used, and numerical R^2 values were displayed directly within heatmap cells to aid in comparative interpretation.

Acknowledgments

We thank the patients' families for donating brain tissues. This work was supported by grants from the National Institutes of Health (NIH) (1RF1AG065407-01A1) (M.I.D. and L.A.J.), the Cure Alzheimer's Fund (M.I.D.), the Hamon Charitable Foundation (M.I.D.), AMED (JP24zf0127012, JP22jm0210097, and JP22wm0425019) (A.K.), an AARG grant from the Alzheimer's Association, a Healey Center ALS Young Scholar Award, and a Mass General Hospital Mussallem Transformative Scholar Award in ALS Research (Y.S.), a Giovanni Armenise-Harvard Foundation award and an internal start-up fund (Y.L.).

bioRxiv preprint doi: https://doi.org/10.64898/2025.12.22.696002; this version posted December 25, 2025. The copyright holder for this preprint (which was not certified by peer review) is the author/funder. All rights reserved. No reuse allowed without permission.

Figures

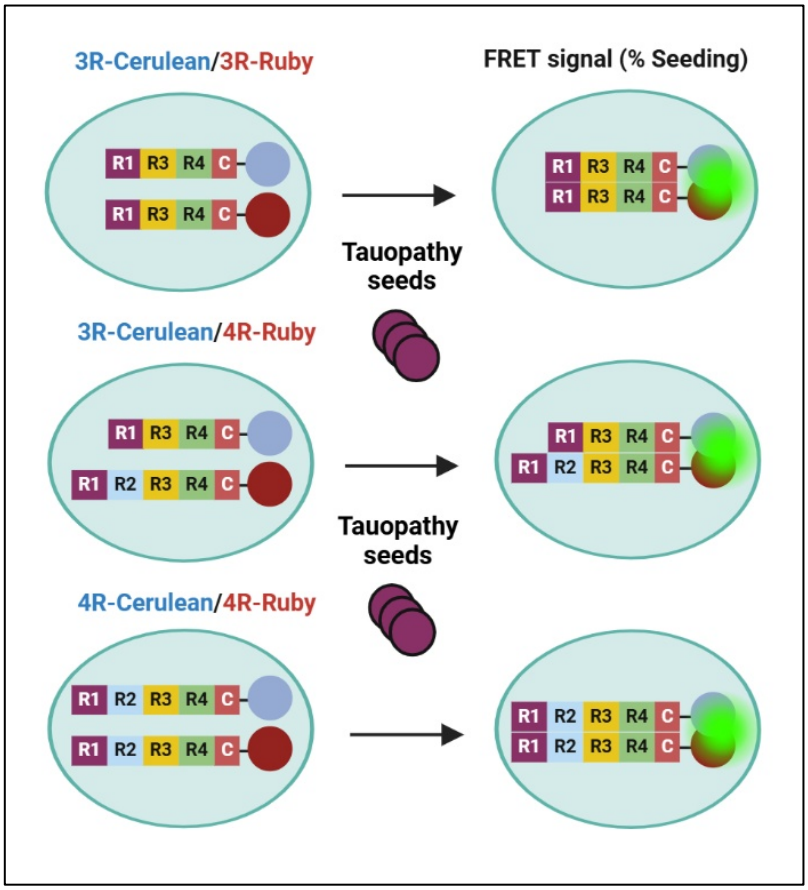


Figure 1: Schematic representation of the tau seeding assay. ALS/PDC nervous tissue extracts were seeded onto biosensor cells containing either 3-repeat (3R) or 4-repeat (4R) tau fused to different fluorophores (Cerulean, Ruby). The three cell lines used harbored 3R tau only (3R/3R), 3R and 4R tau (3R/4R), and 4R tau only (4R/4R). Cells were fixed 72 h post-seeding and evaluated for FRET by flow cytometry.

bioRxiv preprint doi: https://doi.org/10.64898/2025.12.22.696002; this version posted December 25, 2025. The copyright holder for this preprint (which was not certified by peer review) is the author/funder. All rights reserved. No reuse allowed without permission.

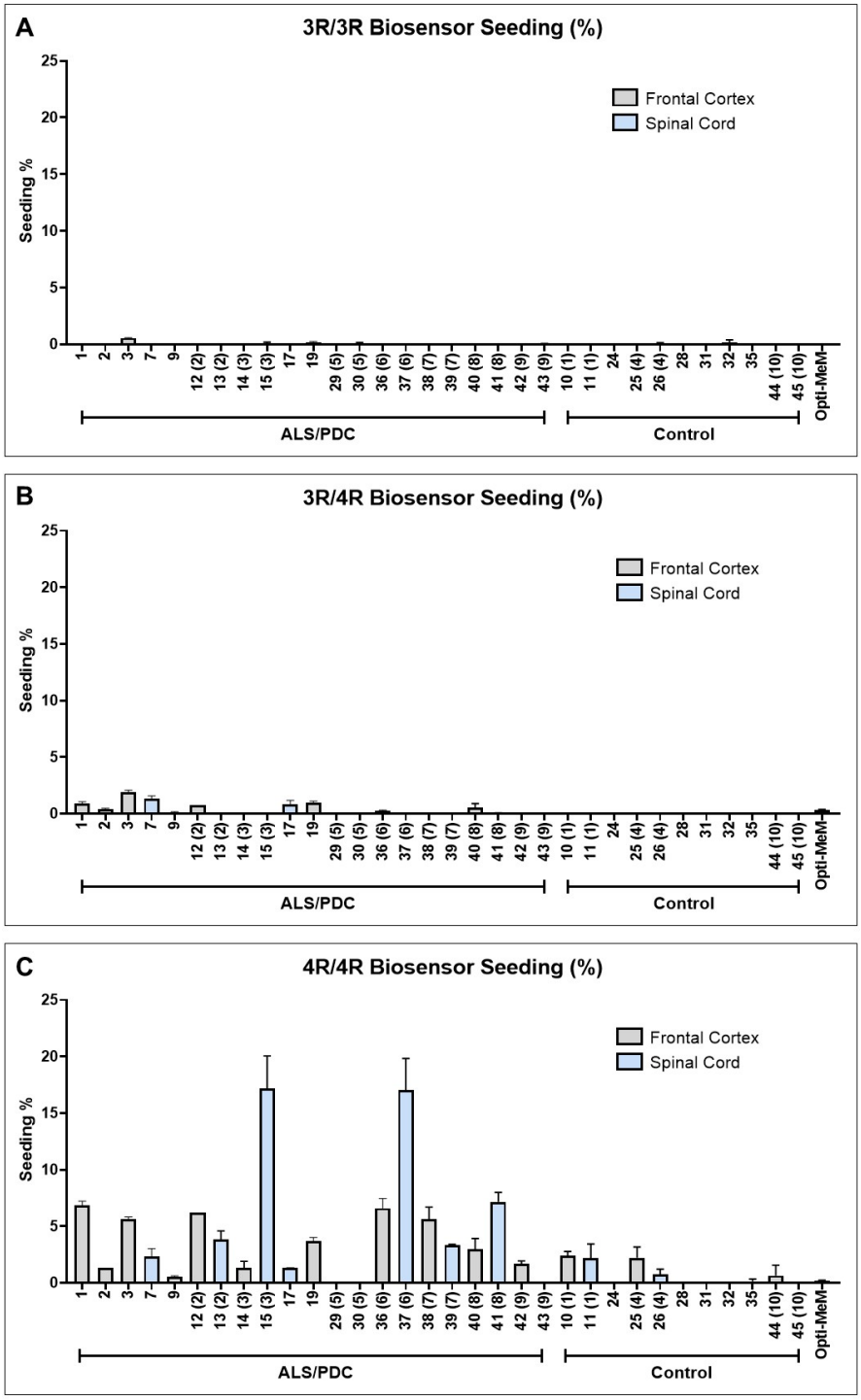


Figure 2: Tau seeds in Guam ALS/PDC brain and spinal cord tissues. 3.5 µg of nervous tissue homogenate material from ALS/PDC cases and Guam controls (Control) were used for the seeding assay. The three cell lines (3R/3R [**A**], 3R/4R [**B**] and 4R/4R [**C**]) were seeded with the homogenates. Quantification of seeding efficiency was made as the % of cells exhibiting FRET signal (Seeding %).

bioRxiv preprint doi: https://doi.org/10.64898/2025.12.22.696002; this version posted December 25, 2025. The copyright holder for this preprint (which was not certified by peer review) is the author/funder. All rights reserved. No reuse allowed without permission.

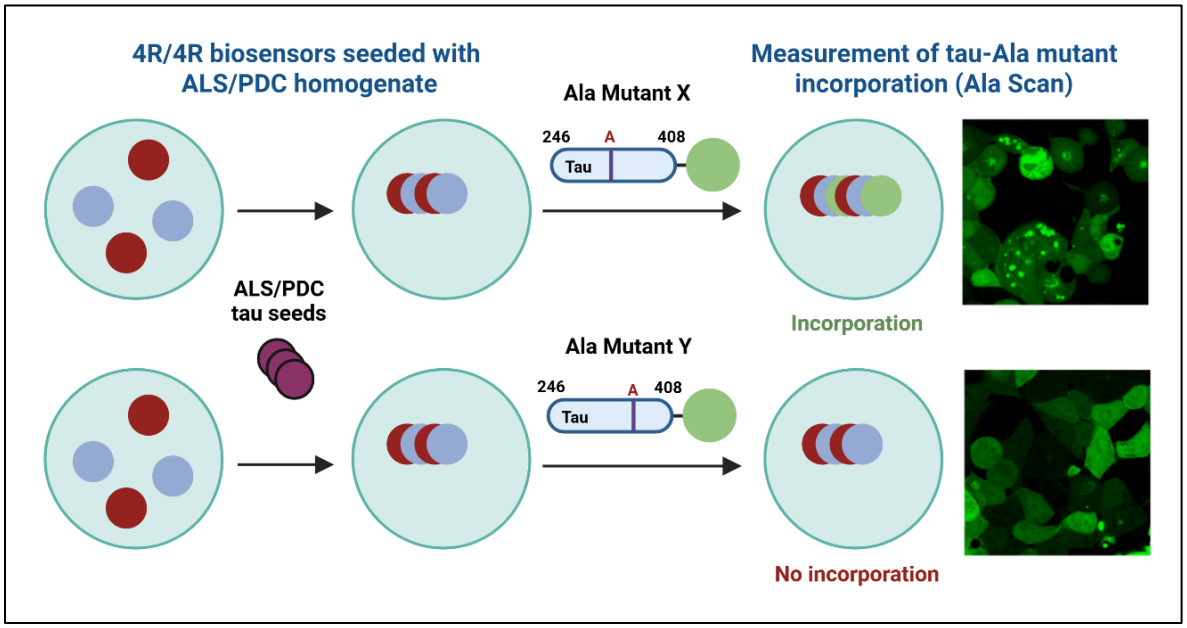


Figure 3: Tau Ala scan overview. The 4R/4R tau biosensor cells were seeded with homogenate from the ALS/PDC cases. After seeding occurred, a lentiviral library of tau Ala point mutants spanning the tau repeat domain (RD) conjugated to fluorophore Clover (i.e. X, Y) was added to the seeded biosensor cells, along with the appropriate controls (wild-type tau RD and I277P-I308P double proline tau RD). Incorporation of each point mutant into the seeded aggregates is measured as the FRET signal between Clover in the Ala point mutants and Cerulean in the cell aggregates. The incorporation profile fingerprint can faithfully discriminate between different tau strains. Figure adapted from (48).

bioRxiv preprint doi: https://doi.org/10.64898/2025.12.22.696002; this version posted December 25, 2025. The copyright holder for this preprint (which was not certified by peer review) is the author/funder. All rights reserved. No reuse allowed without permission.

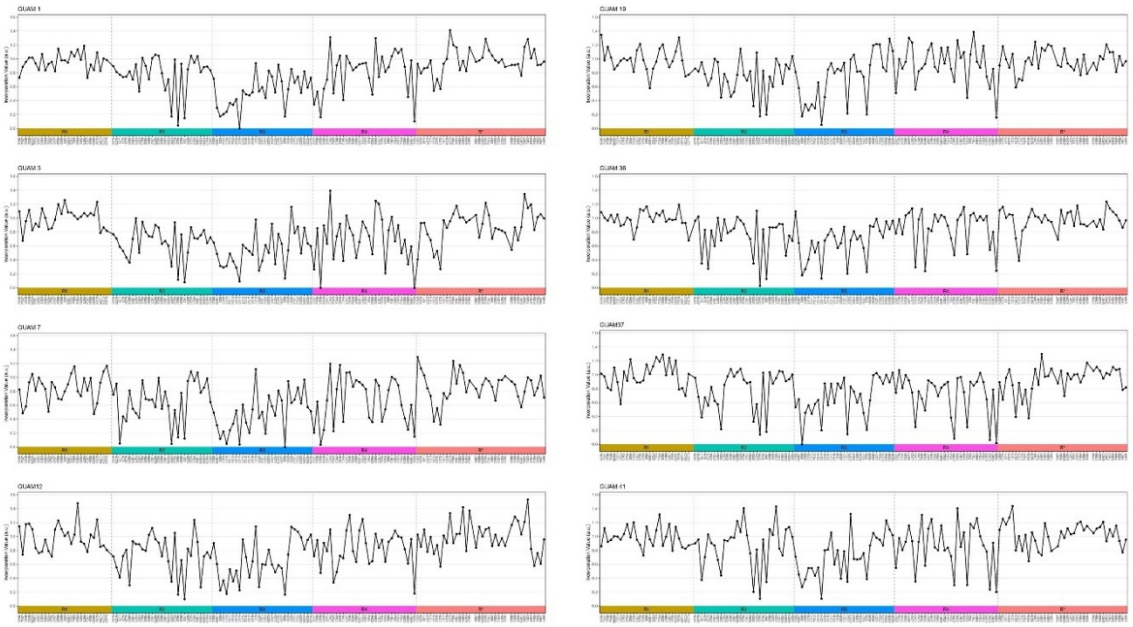


Figure 4: Tau Ala scan of ALS/PDC samples. ALS/PDC brain homogenates from samples #1, #3, #7, #12 (left), #19, #36, #37, and #41 (right) were incubated with the tau 4R/4R biosensor cells. After a 48-hour incubation period that allowed inclusion formation, the biosensor cells were re-plated in triplicates and incubated with the tau-(246-408)-Ala-mEOS3.2 mutant lentivirus library. The cells were harvested 72 hours after transduction. The resulting tau Ala scan is shown for each sample. The incorporation value (a.u.) represents the FRET median fluorescence intensity between Clover and Cerulean for each position normalized by the positive (WT-tau RD- mEOS3.2) and negative controls (I277P-I308P-tau RD-mEOS3.2). Each position in the tau RD is represented on the X axis. Positions K274A, T386A and P397A were excluded from the analysis due to failure of transduction.

bioRxiv preprint doi: https://doi.org/10.64898/2025.12.22.696002; this version posted December 25, 2025. The copyright holder for this preprint (which was not certified by peer review) is the author/funder. All rights reserved. No reuse allowed without permission.

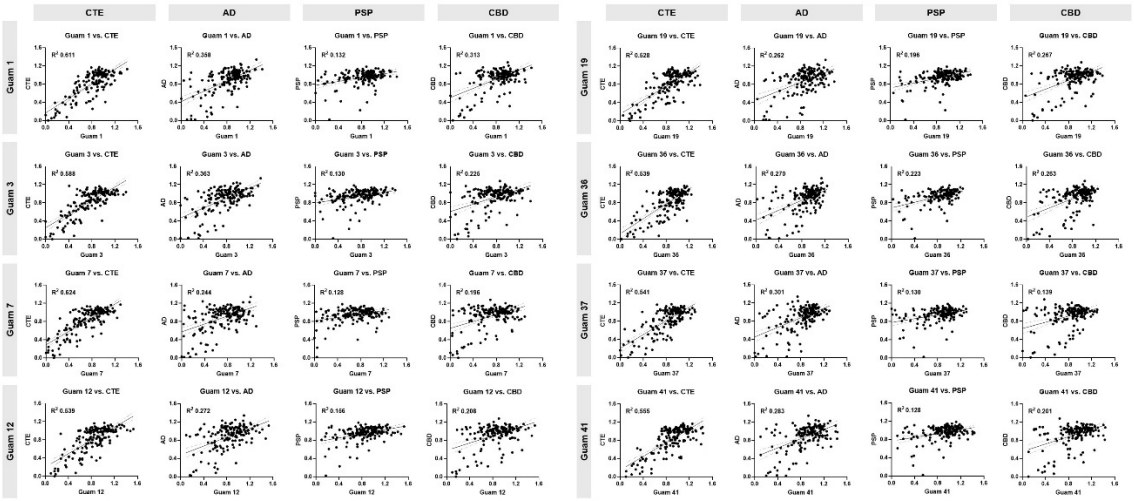


Figure 5: Incorporation profile comparison for ALS/PDC cases. The incorporation profile signature for the ALS/PDC samples was compared with the average incorporation profile of CTE (n=2), AD (n=8), PSP (n=5) and CBD (n=8). The incorporation profile for these samples correlated most closely with the profile in CTE (R^2_{Avg} 0.566 +/- SD 0.037), in comparison to AD (R^2_{Avg} 0.294 +/- SD 0.044), PSP (R^2_{Avg} 0.165 +/- SD 0.039), and CBD (R^2_{Avg} 0.226 +/- SD 0.054).

bioRxiv preprint doi: https://doi.org/10.64898/2025.12.22.696002; this version posted December 25, 2025. The copyright holder for this preprint (which was not certified by peer review) is the author/funder. All rights reserved. No reuse allowed without permission.

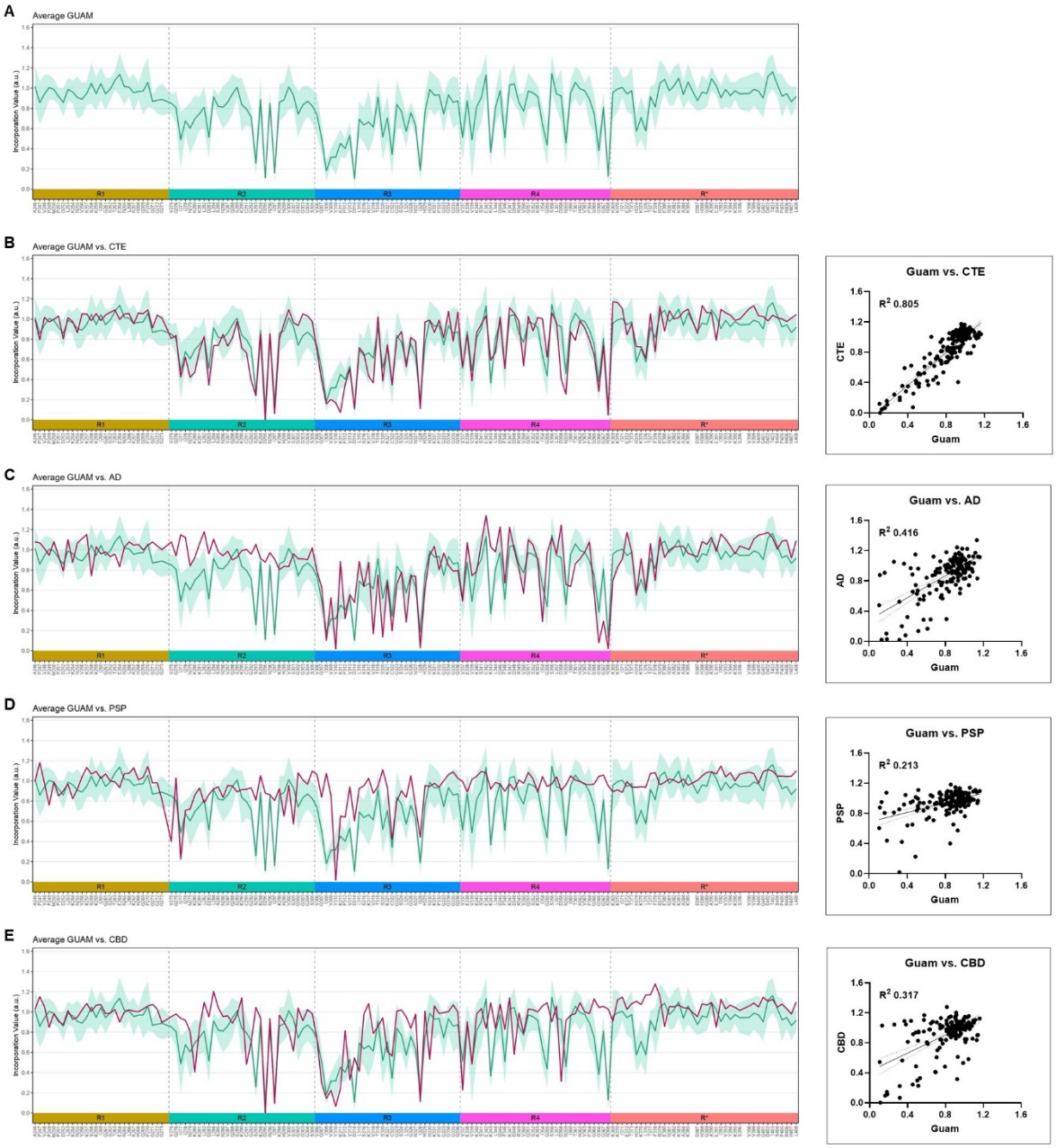


Figure 6: Average incorporation profile for ALS/PDC and comparison with other tauopathy average profiles. A. Mean incorporation profile (line) for the ALS/PDC samples (n=8). The standard deviation (SD) for each position is represented with the teal-colored area. **B**, **C**, **D**, **E**. Comparison of the average ALS/PDC incorporation profile with the average CTE (n=2), AD (n=8), PSP (n=5) and CBD (n=8) profiles. The best correlation was observed with CTE (R^2 0.805).

bioRxiv preprint doi: https://doi.org/10.64898/2025.12.22.696002; this version posted December 25, 2025. The copyright holder for this preprint (which was not certified by peer review) is the author/funder. All rights reserved. No reuse allowed without permission.

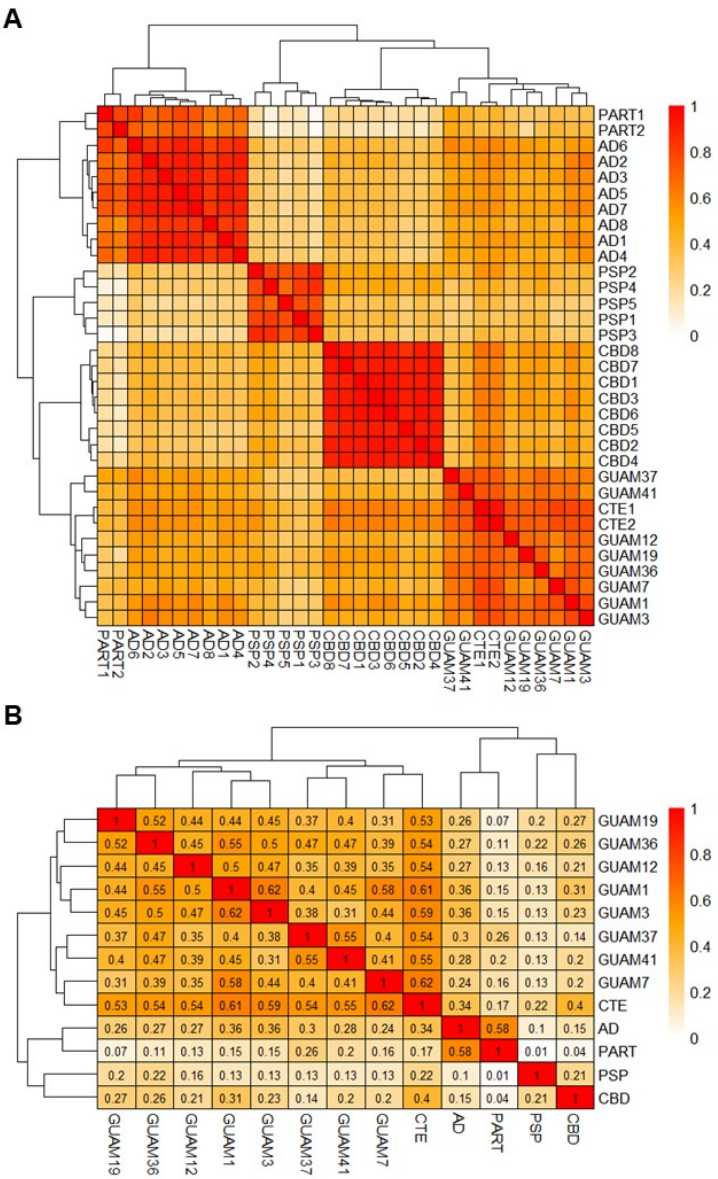


Figure 7: Clustered heatmap analysis of ALS/PDC and other tauopathies. A. Clustered heatmap of ALS/PDC, AD, CTE, CBD, PSP and PART samples. The ALS/PDC samples (GUAM) clustered together with the CTE cases. **B**. Clustered heatmap analysis of ALS/PDC samples and the average profiles for AD (n=8), CTE (n=2), CBD (n=8), PSP (n=5), and PART (n=2). The average correlation between all ALS/PDC samples was R^2 0.44 +/- SD 0.078.

bioRxiv preprint doi: https://doi.org/10.64898/2025.12.22.696002; this version posted December 25, 2025. The copyright holder for this preprint (which was not certified by peer review) is the author/funder. All rights reserved. No reuse allowed without permission.

Table 1.

Table 1: Sample IDs used in the study and average seeding percentage in 3R3R, 3R4R and 4R4R biosensors							
Case #	**Pathology Diagnosis**	**Age**	**Gender**	**Tissue Type**	**3R3R Seeding (%)**	**3R4R Seeding (%)**	**4R4R Seeding (%)**
1	ALS/PDC	69	F	Frontal Cortex	0.01	0.89	6.86
2	ALS/PDC	61	M	Frontal Cortex	0.05	0.06	0.14
3	ALS/PDC	52	F	Frontal Cortex	0.56	1.89	5.64
7	ALS/PDC	71	M	Spinal Cord	0.02	1.30	2.35
9	ALS/PDC	60	M	Frontal Cortex	0.06	0.14	0.26
10 (1)	Control	72	M	Frontal Cortex	0	0	2.42
11 (1)	Control	72	M	Spinal Cord	0	0	2.21
12 (2)	ALS/PDC	54	M	Frontal Cortex	0.03	1.41	4.59
13 (2)	ALS/PDC	54	M	Spinal Cord	0	0	3.86
14 (3)	ALS/PDC	64	F	Frontal Cortex	0	0	1.33
15 (3)	ALS/PDC	64	F	Spinal Cord	0.08	0	17.15
17	ALS/PDC	73	M	Spinal Cord	0	0	8.63
19	ALS/PDC	51	F	Frontal Cortex	0.19	0.99	3.69
24	Control	68	F	Spinal Cord	0	0	0
25 (4)	Control	57	F	Frontal Cortex	0	0	2.22
26 (4)	Control	57	F	Spinal Cord	0.06	0	0.75
28	Control	48	M	Spinal Cord	0	0	0
29 (5)	ALS/PDC	49	M	Frontal Cortex	0	0	0
30 (5)	ALS/PDC	49	M	Spinal Cord	0.07	0	0
31	Control	31	M	Frontal Cortex	0	0	0
32	Control	27	M	Frontal Cortex	0.16	0	0
35	Control	63	M	Spinal Cord	0	0.01	0.14
36 (6)	ALS/PDC	61	M	Frontal Cortex	0	0.26	6.60
37 (6)	ALS/PDC	61	M	Spinal Cord	0	0.04	17.0
38 (7)	ALS/PDC	76	M	Frontal Cortex	0	0.01	5.62
39 (7)	ALS/PDC	76	M	Spinal Cord	0	0.01	3.33
40 (8)	ALS/PDC	69	M	Frontal Cortex	0	0.56	2.97
41 (8)	ALS/PDC	69	M	Spinal Cord	0	0.03	7.16
42 (9)	ALS/PDC	45	M	Frontal Cortex	0	0	1.68
43 (9)	ALS/PDC	45	M	Spinal Cord	0.03	0	0
44 (10)	Control	56	M	Frontal Cortex	0	0	0.65
45 (10)	Control	56	M	Spinal Cord	0	0	0

(N) Sample IDs labelled with a (N) represent provenance from the same case.
Abbreviations: F, Female; M, Male

Table 2.

Table 2: Sample IDs used in the 4R/4R Alanine Scan				
Case #	**Pathology Diagnosis**	**Age**	**Gender**	**Tissue Type**
1	ALS/PDC	69	F	Frontal Cortex
3	ALS/PDC	52	F	Frontal Cortex
7	ALS/PDC	71	M	Spinal Cord
12	ALS/PDC	54	M	Frontal Cortex
19	ALS/PDC	51	F	Frontal Cortex
36 (6)	ALS/PDC	61	M	Frontal Cortex
37 (6)	ALS/PDC	61	M	Spinal Cord
41	ALS/PDC	69	M	Spinal Cord

(N) Sample IDs labelled with a (N) represent provenance from the same case.

bioRxiv preprint doi: https://doi.org/10.64898/2025.12.22.696002; this version posted December 25, 2025. The copyright holder for this preprint (which was not certified by peer review) is the author/funder. All rights reserved. No reuse allowed without permission.

References

1. H. M. Zimmerman (1945) Memorandum to U.S.N. medical research unit No. 2
2. A. Arnold, D. C. Edgren, V. S. Palladino, Amyotrophic lateral sclerosis; fifty cases observed on Guam. *J Nerv Ment Dis* **117**, 135-139 (1953).
3. D. W. Mulder, L. T. Kurland, L. L. Iriarte, Neurologic diseases on the island of Guam. *U S Armed Forces Med J* **5**, 1724-1739 (1954).
4. L. T. Kurland *et al.*, Amyotrophic lateral sclerosis in the Mariana Islands. *AMA Arch Neurol Psychiatry* **75**, 435-441 (1956).
5. A. Hirano, L. T. Kurland, R. S. Krooth, S. Lessell, Parkinsonism-dementia complex, an endemic disease on the island of Guam. I. Clinical features. *Brain* **84**, 642-661 (1961).
6. H. Shiraki, Y. Yase, Eds., *Amyotrophic lateral sclerosis in Japan* (Elsevier, New York, 1975), Vol 22, pp 353–419.
7. S. Kuzuhara, Y. Kokubo, Atypical parkinsonism of Japan: amyotrophic lateral sclerosis-parkinsonism-dementia complex of the Kii peninsula of Japan (Muro disease): an update. *Mov Disord* **20 Suppl 12**, S108-113 (2005).
8. D. C. Gajdusek, A. M. Salazar, Amyotrophic lateral sclerosis and parkinsonian syndromes in high incidence among the Auyu and Jakai people of West New Guinea. *Neurology* **32**, 107-126 (1982).
9. K. Okumiya *et al.*, Amyotrophic lateral sclerosis and parkinsonism in Papua, Indonesia: 2001-2012 survey results. *BMJ Open* **4**, e004353 (2014).
10. J. C. Steele, Parkinsonism-dementia complex of Guam. *Mov Disord* **20 Suppl 12**, S99-S107 (2005).
11. R. M. Garruto, R. Yanagihara, D. C. Gajdusek, Disappearance of high-incidence amyotrophic lateral sclerosis and parkinsonism-dementia on Guam. *Neurology* **35**, 193-198 (1985).
12. C. C. Plato *et al.*, Amyotrophic lateral sclerosis and parkinsonism-dementia complex of Guam: changing incidence rates during the past 60 years. *Am J Epidemiol* **157**, 149-157 (2003).
13. R. M. Garruto, D. C. Gajdusek, K. M. Chen, Amyotrophic lateral sclerosis and parkinsonism-dementia among Filipino migrants to Guam. *Ann Neurol* **10**, 341-350 (1981).
14. A. Hirano, N. Malamud, L. T. Kurland, Parkinsonism-dementia complex, an endemic disease on the island of Guam. II. Pathological features. *Brain* **84**, 662-679 (1961).
15. L. Chen, Neurofibrillary change on Guam. *Arch Neurol* **38**, 16-18 (1981).
16. K. Oyanagi *et al.*, Amyotrophic lateral sclerosis of Guam: the nature of the neuropathological findings. *Acta Neuropathol* **88**, 405-412 (1994).
17. M. Hasegawa *et al.*, TDP-43 is deposited in the Guam parkinsonism-dementia complex brains. *Brain* **130**, 1386-1394 (2007).
18. F. Geser *et al.*, Pathological TDP-43 in parkinsonism-dementia complex and amyotrophic lateral sclerosis of Guam. *Acta Neuropathol* **115**, 133-145 (2008).
19. S. Maekawa *et al.*, TDP-43 is consistently co-localized with ubiquitinated inclusions in sporadic and Guam amyotrophic lateral sclerosis but not in familial amyotrophic lateral sclerosis with and without SOD1 mutations. *Neuropathology* **29**, 672-683 (2009).
20. S. Matsumoto, A. Hirano, S. Goto, Spinal cord neurofibrillary tangles of Guamanian amyotrophic lateral sclerosis and parkinsonism-dementia complex: an immunohistochemical study. *Neurology* **40**, 975-979 (1990).
21. T. Umahara, A. Hirano, S. Kato, N. Shibata, S. H. Yen, Demonstration of neurofibrillary tangles and neuropil thread-like structures in spinal cord white matter in parkinsonism-dementia complex on Guam and in Guamanian amyotrophic lateral sclerosis. *Acta Neuropathol* **88**, 180-184 (1994).

bioRxiv preprint doi: https://doi.org/10.64898/2025.12.22.696002; this version posted December 25, 2025. The copyright holder for this preprint (which was not certified by peer review) is the author/funder. All rights reserved. No reuse allowed without permission.

22. K. Oyanagi *et al.*, Distinct pathological features of the gallyas- and tau-positive glia in the Parkinsonism-dementia complex and amyotrophic lateral sclerosis of Guam. *J Neuropathol Exp Neurol* **56**, 308-316 (1997).
23. M. L. Schmidt *et al.*, Spinal cord neurofibrillary pathology in Alzheimer disease and Guam Parkinsonism-dementia complex. *J Neuropathol Exp Neurol* **60**, 1075-1086 (2001).
24. M. Yamazaki *et al.*, Tau-positive fine granules in the cerebral white matter: a novel finding among the tauopathies exclusive to parkinsonism-dementia complex of Guam. *J Neuropathol Exp Neurol* **64**, 839-846 (2005).
25. M. J. Winton *et al.*, Characterization of tau pathologies in gray and white matter of Guam parkinsonism-dementia complex. *Acta Neuropathol* **111**, 401-412 (2006).
26. P. R. Hof *et al.*, Amyotrophic lateral sclerosis/parkinsonism-dementia complex of Guam: quantitative neuropathology, immunohistochemical analysis of neuronal vulnerability, and comparison with related neurodegenerative disorders. *Acta Neuropathol* **88**, 397-404 (1994).
27. G. G. Kovacs, J. L. Robinson, D. P. Perl, V. M. Lee, J. Q. Trojanowski, Thorn-shaped astrocytes in the depth of cortical sulci in Western Pacific ALS/Parkinsonism-Dementia complex. *Acta Neuropathol* **140**, 591-593 (2020).
28. M. Yamazaki *et al.*, Alpha-synuclein inclusions in amygdala in the brains of patients with the parkinsonism-dementia complex of Guam. *J Neuropathol Exp Neurol* **59**, 585-591 (2000).
29. M. S. Forman *et al.*, Tau and alpha-synuclein pathology in amygdala of Parkinsonism-dementia complex patients of Guam. *Am J Pathol* **160**, 1725-1731 (2002).
30. J. Sebeo, P. R. Hof, D. P. Perl, Occurrence of alpha-synuclein pathology in the cerebellum of Guamanian patients with parkinsonism-dementia complex. *Acta Neuropathol* **107**, 497-503 (2004).
31. K. Oyanagi, T. Hashimoto, M. Yamazaki, "Parkinsonism-dementia complex of Guam." in In: Neurodegeneration: The Molecular Pathology of Dementia and Movement Disorders. (John Wiley & Sons, Ltd, 2011), pp. 171–178.
32. F. H. Anderson, E. P. Richardson, Jr., H. Okazaki, J. A. Brody, Neurofibrillary degeneration on Guam: frequency in Chamorros and non Chamorros with no known neurological disease. *Brain* **102**, 65-77 (1979).
33. D. P. Perl, P. R. Hof, D. P. Purohit, A. J. Loerzel, B. A. Kakulas, Hippocampal and entorhinal cortex neurofibrillary tangle formation in Guamanian Chamorros free of overt neurologic dysfunction. *J Neuropathol Exp Neurol* **62**, 381-388 (2003).
34. M. Mimuro, M. Yoshida, S. Kuzuhara, Y. Kokubo, Amyotrophic lateral sclerosis and parkinsonism-dementia complex of the Hohara focus of the Kii Peninsula: A multiple proteinopathy? *Neuropathology* **38**, 98-107 (2018).
35. M. Goedert, M. G. Spillantini, Propagation of Tau aggregates. *Mol Brain* **10**, 18 (2017).
36. Y. Shi *et al.*, Structure-based classification of tauopathies. *Nature* **598**, 359-363 (2021).
37. J. Vaquer-Alicea, M. I. Diamond, L. A. Joachimiak, Tau strains shape disease. *Acta Neuropathol* **142**, 57-71 (2021).
38. F. Clavaguera *et al.*, Transmission and spreading of tauopathy in transgenic mouse brain. *Nat Cell Biol* **11**, 909-913 (2009).
39. D. W. Sanders *et al.*, Distinct tau prion strains propagate in cells and mice and define different tauopathies. *Neuron* **82**, 1271-1288 (2014).
40. S. K. Kaufman *et al.*, Tau Prion Strains Dictate Patterns of Cell Pathology, Progression Rate, and Regional Vulnerability In Vivo. *Neuron* **92**, 796-812 (2016).

bioRxiv preprint doi: https://doi.org/10.64898/2025.12.22.696002; this version posted December 25, 2025. The copyright holder for this preprint (which was not certified by peer review) is the author/funder. All rights reserved. No reuse allowed without permission.

41. M. Huang, W. A. McEwan, Sensitive detection and propagation of brain-derived tau assemblies in HEK293-based wild-type tau seeding assays. *J Biol Chem* **301**, 108245 (2025).
42. S. H. W. Scheres, B. Ryskeldi-Falcon, M. Goedert, Molecular pathology of neurodegenerative diseases by cryo-EM of amyloids. *Nature* **621**, 701-710 (2023).
43. C. Condello *et al.*, Guam ALS-PDC is a distinct double-prion disorder featuring both tau and Abeta prions. *Proc Natl Acad Sci U S A* **120**, e2220984120 (2023).
44. C. Qi *et al.*, Tau filaments from amyotrophic lateral sclerosis/parkinsonism-dementia complex adopt the CTE fold. *Proc Natl Acad Sci U S A* **120**, e2306767120 (2023).
45. B. Falcon *et al.*, Novel tau filament fold in chronic traumatic encephalopathy encloses hydrophobic molecules. *Nature* **568**, 420-423 (2019).
46. C. Qi *et al.*, Identical tau filaments in subacute sclerosing panencephalitis and chronic traumatic encephalopathy. *Acta Neuropathol Commun* **11**, 74 (2023).
47. C. Qi *et al.*, Tau filaments with the chronic traumatic encephalopathy fold in a case of vacuolar tauopathy with VCP mutation D395G. *Acta Neuropathol* **147**, 86 (2024).
48. J. Vaquer-Alicea *et al.*, Functional classification of tauopathy strains reveals the role of protofilament core residues. *Sci Adv* **11**, eadp5978 (2025).
49. N. Saez-Calveras *et al.*, Essential tremor with tau pathology features seeds indistinguishable in conformation from Alzheimer's disease and primary age-related tauopathy. *Acta Neuropathol* **149**, 6 (2025).
50. J. D. Cherry *et al.*, Tau isoforms are differentially expressed across the hippocampus in chronic traumatic encephalopathy and Alzheimer's disease. *Acta Neuropathol Commun* **9**, 86 (2021).
51. T. Kato, A. Hirano, M. N. Weinberg, A. K. Jacobs, Spinal cord lesions in progressive supranuclear palsy: some new observations. *Acta Neuropathol* **71**, 11-14 (1986).
52. B. N. Dugger *et al.*, The distribution of phosphorylated tau in spinal cords of Alzheimer's disease and non-demented individuals. *J Alzheimers Dis* **34**, 529-536 (2013).
53. A. J. Moszczynski *et al.*, Pathologic Thr(175) tau phosphorylation in CTE and CTE with ALS. *Neurology* **90**, e380-e387 (2018).
54. C. N. Fournier, M. Gearing, J. D. Glass, Tau deposition in the spinal cord is not specific for CTE-ALS. *Neurology* **95**, 37-39 (2020).
55. P. R. Hof, D. P. Perl, A. J. Loerzel, J. H. Morrison, Neurofibrillary tangle distribution in the cerebral cortex of parkinsonism-dementia cases from Guam: differences with Alzheimer's disease. *Brain Res* **564**, 306-313 (1991).
56. C. Schwab, J. C. Steele, H. Akiyama, P. L. McGeer, Distinct distribution of apolipoprotein E and beta-amyloid immunoreactivity in the hippocampus of Parkinson dementia complex of Guam. *Acta Neuropathol* **92**, 378-385 (1996).
57. M. L. Schmidt *et al.*, Amyloid plaques in Guam amyotrophic lateral sclerosis/parkinsonism-dementia complex contain species of A beta similar to those found in the amyloid plaques of Alzheimer's disease and pathological aging. *Acta Neuropathol* **95**, 117-122 (1998).
58. S. M. Gentleman *et al.*, Beta (A4)-amyloid protein and parkinsonian dementia complex of Guam. *Lancet* **337**, 55-56 (1991).
59. H. Ito, H. Hirano, S. H. Yen, S. Kato, Demonstration of beta amyloid protein-containing neurofibrillary tangles in parkinsonism-dementia complex on Guam. *Neuropathol Appl Neurobiol* **17**, 365-373 (1991).
60. D. C. Guiroy *et al.*, Neurofibrillary tangles of Guamanian amyotrophic lateral sclerosis, parkinsonism-dementia and neurologically normal Guamanians contain a 4- to 4.5-kilodalton protein which is immunoreactive to anti-amyloid beta/A4-protein antibodies. *Acta Neuropathol* **86**, 265-274 (1993).

bioRxiv preprint doi: https://doi.org/10.64898/2025.12.22.696002; this version posted December 25, 2025. The copyright holder for this preprint (which was not certified by peer review) is the author/funder. All rights reserved. No reuse allowed without permission.

61. C. Schwab, J. C. Steele, H. Akiyama, E. G. McGeer, P. L. McGeer, Relationship of amyloid beta/A4 protein to the neurofibrillary tangles in Guamanian parkinsonism-dementia. *Acta Neuropathol* **90**, 287-298 (1995).
62. J. Miklossy *et al.*, Enduring involvement of tau, beta-amyloid, alpha-synuclein, ubiquitin and TDP-43 pathology in the amyotrophic lateral sclerosis/parkinsonism-dementia complex of Guam (ALS/PDC). *Acta Neuropathol* **116**, 625-637 (2008).
63. J. L. Furman *et al.*, Widespread tau seeding activity at early Braak stages. *Acta Neuropathol* **133**, 91-100 (2017).
64. A. L. Woerman *et al.*, Kinetics of Human Mutant Tau Prion Formation in the Brains of 2 Transgenic Mouse Lines. *JAMA Neurol* **74**, 1464-1472 (2017).
65. L. Ye *et al.*, Abeta seeding potency peaks in the early stages of cerebral beta-amyloidosis. *EMBO Rep* **18**, 1536-1544 (2017).
66. A. L. Woerman *et al.*, Kinetics of alpha-synuclein prions preceding neuropathological inclusions in multiple system atrophy. *PLoS Pathog* **16**, e1008222 (2020).
67. R. Smith *et al.*, Misfolded alpha-synuclein in amyotrophic lateral sclerosis: Implications for diagnosis and treatment. *Eur J Neurol* **31**, e16206 (2024).